PAPER

Check for updates

Effect of trifluoroacetic acid on InP/ZnSe/ZnS quantum dots: mimicking the surface trap and their effects on the photophysical properties†

Young Mo Sung,[a] Tae-Gon Kim,[b] Dong-Jin Yun,[a] Byeong Gyu Chae,[a] Hyokeun Park,[a] Hyo Sug Lee,[a] Jung-Hwa Kim, [ID][a] Shinae Jun*[b] and Soohwan Sul [ID] *[a]

Understanding the precise effects of defects on the photophysical properties of quantum dots (QDs) is essential to their development with near-unity luminescence. Because of the complicated nature of defects in QDs, the origins and detailed roles of the defects still remain rarely understood. In this regard, we used detailed chemical analysis to investigate the effect of surface defects on the optical properties of InP/ZnSe/ZnS QDs by introducing shell defects through controlled trifluoroacetic acid (TFA) etching. TFA treatment on the InP/ZnSe/ZnS QDs partially removed the ZnS shell as well as ligands and reduced the quantum yield by generating energetically deep surface traps. The surface defects of QDs by TFA cause charged trap sites inducing an Auger recombination process with a rate of *ca.* 200 ps. Based on these results, we proposed possible trap-assisted non-radiative decay pathways between the band-edge state and surface deep traps in InP/ZnSe/ZnS QDs.

Introduction

Semiconductor quantum dots (QDs) having excitonic size smaller than the Bohr radius have gathered increased attention from academia as well as industry owing to their high photoluminescence (PL) quantum yields (QYs), long-term stability, and their potential for use in various applications such as solar cells, photodetectors, and light emitting diodes.[1–6] In particular, InP/ZnSe/ZnS core/shell/shell QDs have significant potential for commercial applications, because they do not contain any toxic elements such as Cd, Pb, or Hg.[7–10] Previously, zinc chalcogenide shells were introduced into InP QDs to obtain highly efficient and chemically stable QDs by confining the excitons within the InP core regions, thereby sheltering them from surface defects and the surrounding environment.[11–15] However, the electron and hole can be delocalized over the shells, and thus, the presence of surface defects has a negative influence on the chemical and physical properties of the QDs.[16,17] Defects related to the shell may originate from factors such as non-uniform shell morphology, surface dangling bonds, oxidation, and impurities,[11–17] which can be formed during the synthesis or post-process or application stages. Moreover, QDs can be

exposed to acidic atmospheres for environmental or biomedical applications.[18–21] The practical applications of QDs in the acidic condition could be as pH sensor and marker which are investigated in various papers.[18–21] Although the development of a number of advanced synthetic methods for QDs have significantly improved their PLQYs,[11–15] these defects remain inevitable in InP-based QDs. Exposure to oxidative or acidic environments during the process or the operation of the electronic or biomedical applications of QDs can be additional sources of surface defects.[20] Despite this significance, the detailed effects of the surface defects in shells on the photophysical properties remain poorly discovered.

In this regard, we synthesized environmentally friendly InP/ZnSe/ZnS QDs which are attractive test beds for biomedical applications due to their nontoxic materials, and investigated their photophysical properties while adding trifluoroacetic acid (TFA) to the QDs, which introduced various surface defects due to ligand removal or the dissolution of surface atoms.[20] Moreover, we have measured the photophysical properties of the QDs at the low temperature and pyridine-added QDs to more sophisticatedly reveal the ligand effect on the surface and the relationship between surface defects and deep trap.

To understand the photophysical characteristics of TFA-treated QDs, chemical and morphological properties were characterized using inductively coupled plasma atomic emission spectroscopy (ICP-AES), X-ray photoelectron spectroscopy (XPS), and transmission electron microscopy (TEM) (Fig. 1 and S1–S4†). The pristine QDs have a diameter of ~4.6 nm measured by TEM, which is consistent with the 4.5 nm estimated by ICP-AES with a core diameter of 2.1 nm and each shell

[a]Analytical Engineering Group, Samsung Advanced Institute of Technology, 130, Samsung-ro, Yeongtong-gu, Suwon-si, Gyeonggi-do, 16678, South Korea. E-mail: soohwan.sul@samsung.com

[b]Organic Materials Lab, Samsung Advanced Institute of Technology, 130, Samsung-ro, Yeongtong-gu, Suwon-si, Gyeonggi-do, 16678, South Korea

† Electronic supplementary information (ESI) available. See DOI: https://doi.org/10.1039/d3ra05441a
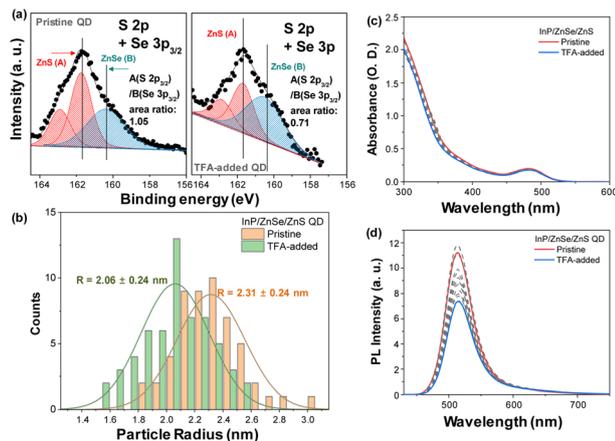
Fig. 1 TFA etches the shell of QDs, which affect their steady-state results. (a) X-ray photoelectron spectroscopy (XPS) results and (b) size distribution from Transmission electron microscopy (TEM) images of pristine and trifluoroacetic acid (TFA)-added quantum dots (QDs). (R^2 for size distribution fitting of pristine and TFA-added QDs are 0.942 and 0.884, respectively.) The (c) absorption and (d) photo-luminescence (PL) spectra of InP/ZnSe/ZnS QDs with increasing the amount of TFA added.

thickness of 0.6 nm for ZnSe and ZnS. Then we added excess amounts of TFA to the QDs, TEM images showed the size distribution with a central position at ~4.1 nm (Fig. 1 and Fig. S2†). XPS analysis in Fig. 1 reveals that the chemical composition of ZnS to ZnSe significantly decreased as a result of the TFA addition (1.06 → 0.71). Moreover, a significant proportion of the passivated ligand observed in gas chromatography (GC) was removed by TFA treatment (Fig. S5†). Unlike ZnS and ligand components, the ZnSe layer remained intact, which was well protected by the outer layers (See C 1s and Se 3d core levels in Fig. S3 and S4†). Thus, the TFA-treated QDs in this study are good candidates for revealing only the surface effect without additional effects such as ZnSe interlayer. These chemical and physical analyses indicate that the TFA corrodes the shell of the QDs, especially for the ZnS shell and ligands of the QDs, inducing surface defects on the QDs.

Results and discussion

To observe the effect of TFA on the photophysical properties of the QDs, we investigated the steady-state absorption and PL spectra by adding TFA to the solution. The absorption spectra of the QDs present spectral features of typical green-emitting QDs with the first excitonic band at 482 nm and strong absorption from ZnSe and ZnS shells for wavelength <400 nm (Fig. 1).[11–15] Upon the addition of TFA, the absorption spectra of the QDs exhibited similar intensities at the first excitonic peak with a slight decrease in absorption from ZnS shells for wavelength <400 nm. Tauc plots of pristine and TFA-added QDs estimated by their absorption spectra show similar band gaps and spectral features (Fig. S6†). In both the presence and absence of TFA, the PL spectra of the QDs exhibited similar spectral shapes with sharp band-edge emission at 514 nm with a smeared band for

wavelength between 600 and 700 nm. However, the PL intensity of the QDs reduced with increasing TFA concentration (Fig. 1) and the PLQY of QDs decreased from 0.80 to 0.55 upon the addition of TFA (Fig. S7†).

With decreasing PL intensity in TFA-added QDs, the time-resolved photoluminescence (TRPL) spectra exhibited distinct changes upon the addition of TFA to the QDs (Fig. S7†–S9). More specifically, upon the addition of TFA to the QDs, fast components (sub 10 ns) were newly observed and the ratio of the slow components (>100 ns) increased. Although these fast components were newly observed upon the addition of TFA, the average lifetimes of the TFA-added QDs were found to be similar to those of the pristine QDs, because the portion of slow components increased as well (Fig. S5 and S8†). The time-resolved emission spectra (TRES) of the pristine and TFA-added QDs clearly indicate the increased fast and slow components in the TFA-added QDs (Fig. 2). The TRES of the pristine QDs was fitted with two-time components, 40 and 100 ns, while the TRES of TFA-added QDs consisted of three species with sub-10, 40, and 120 ns. Considering the timescale and the TRES features of pristine QDs, we suggested that the time component of 40 ns originates from the band-edge emission, while the ≥100 ns component was associated with the trap emission that possessed a lower intensity than the band-edge emission. However, the additionally observed sub-10 ns component of TFA-added QDs in the TRES exhibited higher energy level than that of the band-edge emission, which suggested that the fast term may not be simply associated with the trap emission.

To rationalize the fast component in the TRPL of the TFA-added QDs, we estimated the radiative and non-radiative rates. As the amount of TFA added to the QD solution increased, the radiative and non-radiative rates of the QDs decreased and increased, respectively (Fig. S7†). The increased non-radiative rates were primarily attributed to the newly
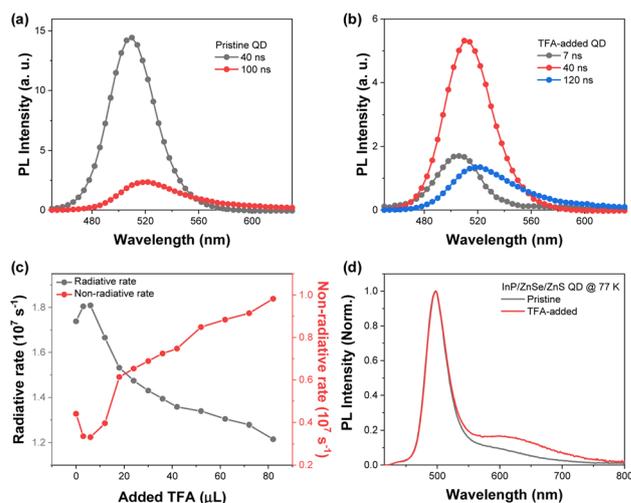
Fig. 2 Time-resolved emission spectra (TRES) of (a) pristine and (b) TFA-added QDS, (c) radiative and non-radiative rates of InP/ZnSe/ZnS QDs with increasing amounts of TFA. The (d) photoluminescence (PL) spectra of pristine and TFA-added QDs at 77 K.

appeared fast component of TFA-added QDs.[16,17] Considering the XPS and TEM results that indicate the peeling of the ZnS shell from the QDs by TFA, the fast decay components of approximately 10 ns were attributed to the presence of the surface defects on the ZnS shell.

To obtain more detailed information regarding the trap emission, the PL spectra at low temperatures showing distinct band-edge and trap emission were measured.[22] The PL spectra of the pristine QD at 77 K exhibited relatively sharp and blue-shifted spectra with increasing broad band around 600 nm compared to that at 293 K. When we added TFA to the QDs, the PL spectrum at 77 K exhibited an increased intensity of the smeared band around 620 nm, which illustrates the increased trap emission in the TFA-added QDs. When we fitted the PL spectra with three Gaussian graphs, band-edge, trap1, and trap2 emissions, TFA-added QDs exhibited significantly increased trap2 emission compared to the pristine QDs (Fig. S10†). Considering the energy difference from the band-edge emission and spectral shape, the trap1 emission could be assigned to the shallow trap, and the trap2 emission to the deep trap. The PL spectra of the pristine QDs at 77 K exhibited a 46 : 28 : 26 area ratio among the three Gaussian spectra, while the PL spectra of the TFA-added QDs at 77 K exhibited a 36 : 22 : 43 area ratio. The ratio of the deep trap emission of the TFA-added QDs compared to that of the pristine QDs increased from 26% to 43%. In contrast, the ratio between the band-edge and shallow trap emissions for the pristine and TFA-added QDs were comparable (62 : 38, Fig. S10†). From these results, we can infer that the surface defects on the ZnS shell induced by the TFA etching primarily generated the deep trap emission rather than the shallow trap emission.

The transient absorption (TA) results also exhibited significant differences between the pristine and TFA-added QDs (Fig. 3). The TA results of the pristine QDs exhibited ground state bleaching (GSB) band at 487 nm with broad excited state absorption spectra for wavelength >600 nm. In the case of the TFA-added QDs, the TA spectra present a slightly broadened GSB with the faster decaying spectral features, which was primarily affected by the trap states of TFA-added QDs (Fig. 3). This result is in line with the results from the TRES that showed an increase in the ratio of trapping components. The decay profiles at 488 nm exhibit a clear difference between the pristine and TFA-added QDs. The decay profiles of the pristine QDs depict two decay components, ∼5 ps and >20 ns. In contrast, those of the TFA-added QDs exhibited three decay components, an additional 250 ps term, along with two components observed in the pristine QDs, and the increased contribution of the ∼5 ps (Fig. S11 and S12†).

To reveal the origin of this new component, 250 ps in the TA results of the TFA-added QDs, we investigated their decay profiles by changing the excitation power.[23–30] While both pristine and TFA-added QDs show a simple linear dependence for the 5 ps component ratio as a function of excitation power, there is a tremendous difference in the 250 ps component ratio between the pristine and TFA-added QDs as in Fig. 3.

The 250 ps component of TFA-added QDs show linear dependency on the excitation pump power, which implies that
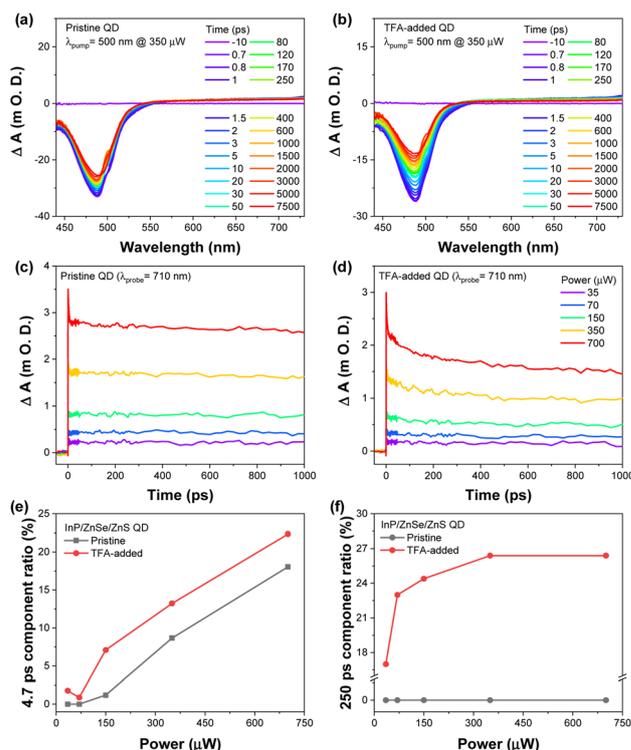

Fig. 3 Power-dependent behavior of TA results illustrates that the time components with sub 10 ps and 250 ps relate to the Auger recombination process. Transient absorption (TA) spectra of the (a) pristine and (b) TFA-added QDs. Decay profiles (c and d) and ratio of the decay components (e and f) of the pristine and TFA-added QDs with changing pump fluence.

the 250 ps component is connected to the Auger recombination process. Considering that the 250 ps component is observed only in the TFA-added QDs which are surface damaged and the trion Auger recombination process of InP QDs takes place with hundreds picosecond scale,[8,23,31,32] the 250 ps could be related to the trion Auger recombination process by surface damage. In other words, TFA treatment causes the trion Auger recombination process by surface damage of InP/ZnSe/ZnS QDs which can accelerate the non-radiative rates of the exciton.[8,23,31,32] In contrast, the ∼5 ps decay dynamics can be attributed to the Auger-assisted carrier trapping.[32–36] Moreover, the ∼5 ps component ratio of TFA-added QDs depending on the pump power exhibited a similar tendency to that of the pristine QDs (Fig. 3). This indicated that the fast decay component (∼5 ps) can be attributed to the different types of trapping dynamics rather than the Auger recombination by the surface defects. By all accounts, the deep trap states of QDs induced by TFA may be associated with surface trion Auger recombination as well as the non-emissive recombination that reduced the PLQYs.[8,23,31,32]

As evaluated from the TEM and XPS analyses, TFA treatment induced the detachment of organic ligands and partial loss of ZnS shell.[36,37] Ligand detachment was additionally confirmed by sensitivity-calibrated GC as depicted in Fig. S5.† To scrutinize the effect of the ligand removal on the photophysical properties, we prepared pyridine-treated QDs with oleic acid (OA) ligands,
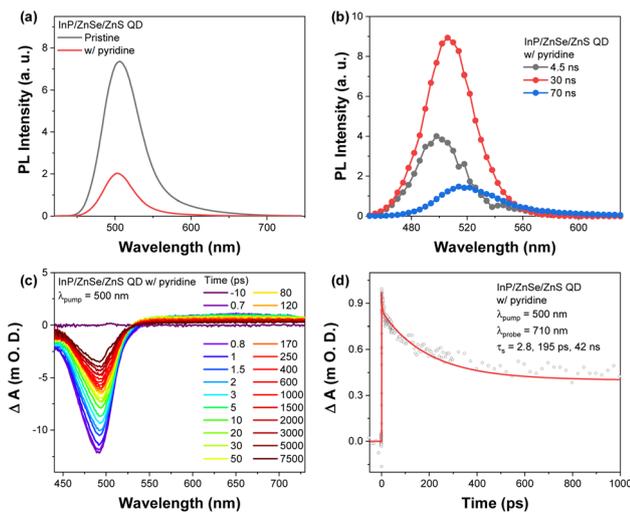
Fig. 4 Pyridine substitution of QD ligand reduced the PL intensity, which is caused by the Auger recombination process by surface charge trap states. (a) PL spectra of the pristine and pyridine-substituted InP/ZnSe/ZnS QDs. (b) TRES of pyridine-substituted InP/ZnSe/ZnS QDs. The (c) TA spectra and (d) decay profiles of the pyridine-substituted InP/ZnSe/ZnS QDs.

as pyridine is an effective amine agent for Z-type displacement of the zinc carboxylate on the surface of QDs.[38–43] The absorption spectra of pyridine-treated QDs showed no specific changes, but their PL spectra exhibited significant decreases, suggesting that the pyridine treatment could affect only the ligand on the surface without any significant removal of the ZnS/ZnSe shell substance (Fig. S13† and Fig. 4). PL lifetimes of the QDs were reduced due to the emergence of the fast component in the pyridine-treated QDs (4.5 ns, Fig. 4 and S14†). TA results of the pyridine-treated QDs reveal similar behavior to those of TFA-added QDs fitted with triple exponential function with three decay components, 2.8, 195, and 42 000 ps. The advent of 195 ps component is close to the observation in TFA-added QDs, that is, surface trion Auger recombination related 250 ps terms observed in TFA-added QDs could have a similar chemical origin to that of pyridine-treated QDs, hole trap states by the S-dangling bond on the ZnS surface.[41–44] This finding suggests that the defects caused by TFA treatment may have a similar chemical nature to the detachment of Zn-oleate (Fig. S11†).

Conclusions

To summarize, TFA etched both the organic ligands and the inorganic shells of InP/ZnSe/ZnS QDs and consequently damaged the surface of QDs. This decreased their PL intensity through the formation of defects related to the detachment of ligand as well as the loss of shells. Increased trap states by TFA treatment were depicted in the PL spectrum at 77 K. The removal of ligands led to the surface trion Auger process by surface charged trap states, while other defects related to the inorganic shell damages contributed to the fast trapping around 5 ps. These results provided clues for the origin of the trap emissions in InP/ZnSe/ZnS QDs, which could be the critical information required for controlling the PL properties of QDs by modifying their shell defects.[45–47]

Author contributions

Y. M. Sung, T.-G. Kim and S. Sul designed the experiment, and analysed the data. Y. M. Sung, T.-G. Kim, D.-J. Yun, B. G. Chae and H. Park performed the experiments (XPS, TEM, GC, spectroscopic measurements and synthesis of QDs). H. S. Lee, J.-H. Kim, S. Jun and S. Sul supervised the project. Y. M. Sung, T.-G. Kim and S. Sul wrote the manuscript. All authors discussed the results and commented on the manuscript.

Conflicts of interest

There are no conflicts to declare.

Acknowledgements

Notes and references

1 A. P. Alivisatos, *Science*, 1996, **271**, 933.
2 V. I. Klimov and D. W. McBranch, *Phys. Rev. B: Condens. Matter Mater. Phys.*, 1997, **55**, 13173.
3 V. I. Klimov and D. W. McBranch, *Phys. Rev. Lett.*, 1998, **80**, 4028.
4 V. I. Klimov, A. A. Mikhailovsky, D. W. McBranch, C. A. Leatherdale and M. G. Bawendi, *Science*, 2000, **287**, 1011.
5 D. V. Talapin, J.-S. Lee, M. V. Kovalenko and E. V. Shevchenko, *Chem. Rev.*, 2010, **110**, 389.
6 C.-H. M. Chuang, P. R. Brown, V. Bulović and M. G. Bawendi, *Nat. Mater.*, 2014, **13**, 796.
7 Y. Li, *et al.*, *J. Am. Chem. Soc.*, 2019, **141**, 6448.
8 Y. Moon, S. Si, E. Yoon and S. J. Kim, *J. Appl. Phys.*, 1998, **83**, 2261.
9 D. Mocatta, *et al.*, *Science*, 2011, **332**, 77.
10 P. Reiss, M. Carrière, C. Lincheneau, L. Vaure and S. Tamang, *Chem. Rev.*, 2016, **116**, 10731.
11 A. Veamatahau, *et al.*, *Phys. Chem. Chem. Phys.*, 2015, **17**, 2850.
12 A. J. Almeida, *et al.*, *J. Phys. Chem. C*, 2016, **120**, 13763.
13 J. Hensel, G. Wang, Y. Li and J. Z. Zhang, *Nano Lett.*, 2010, **10**, 478.
14 J. Wang, *et al.*, *J. Am. Chem. Soc.*, 2013, **135**, 15913.
15 A. Salant, *et al.*, *ACS Nano*, 2010, **4**, 5962.
16 J. v. Embden, J. Jasieniak and P. Mulvaney, *J. Am. Chem. Soc.*, 2009, **131**, 14299.
17 M. Rafipoor, *et al.*, *J. Chem. Phys.*, 2019, **151**, 154704.
18 A. Pavlicek, S. Neubauer, C. Zafiu, M. Huber-Humer, E.-K. Ehmoser and F. Part, *Environ. Pollut.*, 2023, **317**, 120461.

19 C. Zhu, *et al.*, *Prog. Nat. Sci.: Mater. Int.*, 2019, **29**, 628.

20 M. J. Ruedas-Rama, A. Orte, E. A. H. Hall, J. M. Alvarez-Pez and E. M. Talavera, *Chem. Commun.*, 2011, **47**, 2898.

21 D. Herrera-Ochoa, P. J. Pacheco-Liñán, I. Bravo and A. Garzón-Ruiz, *ACS Appl. Mater. Interfaces*, 2022, **14**(2), 2578.

22 V. Babentsov and F. Sizov, *Opto-Electron. Rev.*, 2008, **16**, 208.

23 Y. Kobayashi, T. Nishimura, H. Yamaguchi and N. Tamai, *J. Phys. Chem. Lett.*, 2011, **2**, 1051.

24 M. C. Beard, *J. Phys. Chem. Lett.*, 2011, **2**, 1282.

25 A. V. Malko, A. A. Mikhailovsky, M. A. Petruska, J. A. Hollingsworth and V. I. Klimov, *J. Phys. Chem. B*, 2004, **108**, 5250.

26 P. Tyagi and P. Kambhampati, *J. Chem. Phys.*, 2011, **134**, 094706.

27 J. I. Saari, *et al.*, *J. Phys. Chem. B*, 2013, **117**, 4412.

28 F. García-Santamaría, *et al.*, *Nano Lett.*, 2011, **11**, 687.

29 H. Zhu, *et al.*, *Nano Lett.*, 2014, **14**, 1263.

30 A. F. Richter, *et al.*, *ACS Nano*, 2019, **13**, 14408.

31 I. S. Hauksson, *et al.*, *J. Cryst. Growth*, 1996, **159**, 329.

32 J. M. Pietryga, *et al.*, *Chem. Rev.*, 2016, **116**, 10513.

33 A. W. Cohn, A. M. Schimpf, C. E. Gunthardt and D. R. Gamelin, *Nano Lett.*, 2013, **13**, 1810.

34 S. C. Boehme, *et al.*, *Nano Lett.*, 2015, **15**, 3056.

35 M. Califano, *ACS Nano*, 2015, **9**, 2960.

36 J. Tang, *et al.*, *Nat. Mater.*, 2011, **10**, 765.

37 K. S. Jeong, *et al.*, *ACS Nano*, 2012, **6**, 89.

38 G. H. Woehrle, L. O. Brown and J. E. Hutchison, *J. Am. Chem. Soc.*, 2005, **127**, 2172–2183.

39 I. Moreels, J. C. Martins and Z. Hens, *ChemPhysChem*, 2006, **7**, 1028.

40 E. Zillner, *et al.*, *J. Phys. Chem. C*, 2012, **116**, 16747.

41 N. C. Anderson, M. P. Hendricks, J. J. Choi and J. S. Owen, *J. Am. Chem. Soc.*, 2013, **135**, 18536.

42 C. L. Hartley, M. L. Kessler and J. L. Dempsey, *J. Am. Chem. Soc.*, 2021, **143**, 1251.

43 E. Drijvers, J. D. Roo, J. C. Martins, I. Infante and Z. Hens, *Chem. Mater.*, 2018, **30**, 1178.

44 N. Kirkwood, *et al.*, *J. Am. Chem. Soc.*, 2018, **140**, 15712.

45 A. J. Nozik, *Nanostruct*, 2002, **14**, 115.

46 I. Gur, N. A. Fromer, M. L. Geier and A. P. Alivisatos, *Science*, 2005, **310**, 462.

47 Y. M. Sung, *et al.*, *Small*, 2021, **17**, 2102792.